The European Research Journal 2023;9(1):131-139 Original Article

DOI: 10.18621/eurj.998503 *Medical Biology*

The effects of gold nanoparticles with different surface coatings and sizes on biochemical parameters in mice

İlyas Özçiçek[1, 2], Çağrı Çakıcı[3], Neşe Ayşit[1, 2], Ümit Can Erim[4]

[1]Department of Medical Biology, Istanbul Medipol University School of Medicine, Istanbul, Turkey; [2]Health Science and Technologies Research Institute (SABITA), Istanbul Medipol University, Istanbul, Turkey; [3]Department of Medical Biochemistry, Istanbul Medipol University School of Medicine, Istanbul, Turkey; [4]Department of Analytical Chemistry, Istanbul Medipol University School of Pharmacy, Istanbul, Turkey

ABSTRACT

Objectives: Gold nanoparticles are very popular metallic nanomaterials and they have a wide spectrum of biomedical applications. This study was aimed to the production of stable and monodisperse polyethyleneimine (PEI) and polyethylene glycol (PEG) coated gold nanoparticles (AuNP20 and AuNP50), investigation of their in vivo biochemical effects in the BALB/c mice.

Methods: Gold nanoparticles were synthesized and their surfaces were modified by PEI and PEG. All the necessary physicochemical characterizations were performed. After the single high dose i.v. injection (5 mg Au/kg animal weight) of the AuNP groups, their in vivo biochemical effects were evaluated multiparametrically in the mice on day 14.

Results: Highly monodisperse and stable AuNPs were synthesized successfully. Significant changes in the biochemical hemogram parameters were observed depending on the surface coatings of the AuNPs. PEI and PEG surface coatings increased biocompatibility. No excessive oxidative stress response was observed in all the gold nanoparticle groups.

Conclusions: It has been concluded that the surface chemistry of the particles is a more decisive parameter than the size in terms of in vivo biochemical toxicity. The surface functionalization, stability and biocompatibility of the AuNPs are important parameters for the potential biomedical applications of gold nanoparticles in future studies.

Keywords: Gold nanoparticle, hemogram, nanotoxicity, oxidative stress, PEI/PEG surface coatings

Due to their unique chemical and physical properties, gold nanoparticles (AuNPs) have a wide range of applications in the biomedical field [1]. With the development of more innovative and effective nanomaterial designs, AuNPs have been widely preferred in biomedical research recently, with applications that include antibacterial studies [2], biosensors [3], detection systems [4], imaging [5], DNA/RNA delivery [6, 7], drug delivery [8], photothermal therapy [9] and targeted therapy [10]. The synthesis method, surface coating, size of the nanomaterials, duration and concentration of the exposure play a decisive role on the toxicity of the nanoparticles [11].

In some *in vitro* studies in the literature, it has been shown that gold nanoparticles without surface functionalization were clustered in larger endosomes in the cells by forming aggregates. It has also been reported that generally smaller particles cause more cellular

Received: ***September 21, 2021;*** *Accepted:* ***April 26, 2022;*** *Published Online:* ***June 27, 2022***

How to cite this article: *Özçiçek İ, Çakıcı Ç, Ayşit N, Erim ÜC. The effects of gold nanoparticles with different surface coatings and sizes on biochemical parameters in mice. Eur Res J 2023;9(1):131-139. DOI: 10.18621/eurj.998503*

e-ISSN: 2149-3189

Address for correspondence: *Ilyas Ozcicek, PhD., Assistant Professor, Istanbul Medipol University School of Medicine, Department of Medical Biology, Göztepe Mah., Atatürk Cad., No: 40/16, 34815 Beykoz, Istanbul, Turkey. E-mail: ozcicek@medipol.edu.tr, ilyasozcicek@gmail.com, GSM: +90 546 422 52 06*

toxic effects. It has been reported that PEG-coated gold nanoparticles including small ones, do not cause cellular toxic effects. In addition, it has been shown that particles are localized to smaller endosomes, reduced aggregation and increased cellular particle uptake, thanks to the PEG coating. In the literature, it has been evaluated that PEI surface coating improves cellular nanoparticle uptake, stability and biocompatibility. Under controlled synthesis conditions, a thin layer of low molecular weight PEI surface coating increases the stability of the particles and provides a positive charge [12-19].

Previous in vivo studies have been conducted to evaluate the toxicity and biochemical effects of different gold nanoparticles. It has been demonstrated that the PEG coated various gold nanoparticles increase the stabilization and circulation time in the blood and reduce toxicity [20]. Researchers have shown that smaller nanoparticles lead to more toxic effects and excessive oxidative stress production [21]. Further in vivo studies are needed to determine the biochemical effects of the various gold nanoparticles and their role in nanotoxicity.

This study was aimed to the production of stable and monodisperse polyethyleneimine (PEI, positively charged) and polyethylene glycol (PEG, slightly negatively charged) coated gold nanoparticles (AuNP20 and AuNP50), investigation of their in vivo biochemical effects in the BALB/c mice. Thus, in addition to conventionally synthesized citrate stabilized gold nanoparticles, AuNP variations with different surface chemistries and charges were obtained. In addition, considering the two different AuNP sizes, biochemical effects of various physicochemical parameters of the particles were evaluated apart from the literature.

METHODS

Gold Nanoparticles Synthesis, Surface Functionalization and Characterization

As a first stage, gold seed nanoparticles ($AuNP_{20}$) were synthesized and used in the synthesis of gold nanoparticles with average size ($AuNP_{50}$) in the following stages. Seed AuNPs were produced by modifying the Turkevich synthesis method [22]. Briefly, after 100 ml, 0.25 mM chloroauric acid ($H[AuCl_4]$) solution (Sigma-Aldrich) was prepared, the trisodium citrate dihydrate (reducing agent, Sigma-Aldrich) solution was added at a concentration of 0.033% by increasing the rotational speed of the boiling solution. After the prepared seed AuNP solution was cooled, it was centrifuged (Thermo-Scientific, MicroCL 21R) at 7,000 g for 30 min. Then, it was dispersed in deionized water. AuNPs of 50 nm size were synthesized by the seeding-growth method [23]. 100 ml of 0.25 mM chloroauric acid solution was prepared again, then 2.4 ml of seed AuNPs were added to the solution and mixed at medium rotational speed. Trisodium citrate was added at a concentration of 0.15 mM, and 1 ml of 25 mM hydroquinone (Sigma-Aldrich) solution was added and mixed for 10 min. In the next step, the synthesized AuNPs of 50 nm size were centrifuged at 7000 g for 30 min and then dispersed in deionized water.

For the purpose of PEI coating of all the AuNPs, 2% PEI (Mw: 10000-25000, Sigma-Aldrich) stock solution was prepared and it was added to the AuNPs solution at 0.005% final concentration and mixed for 1 h [17]. After the PEI coating, all the AuNPs solutions were centrifuged at 7000 g for 30 min and then dispersed in deionized water. For the purpose of PEG coating of all the AuNPs, 0.15 mM PEG-SH (Mw: 5000, Nanocs) solution was prepared and 100 µl of the solution was added to each ml of the synthesized AuNPs solution and mixed for 1 h. After the PEG coating, all the AuNPs solutions were centrifuged at 7000 g for 30 min and then dispersed in deionized water [18].

Inductively coupled plasma mass spectrometry (ICP-MS) measurements were applied (Perkin Elmer ICP-MS, Nexion 300X) to precisely quantify the amount of the gold (Au) in all the synthesized AuNPs solutions. For subsequent *in vivo* studies, all the AuNPs solutions were standardized to contain gold (Au) at 500 µg ml^{-1} concentrations. All the synthesized AuNPs were characterized regarding size and zeta potential using a zeta-sizer (Zetasizer Ultra-Malvern). Scanning electron microscope (SEM) images were taken (SEM-Zeiss Geminisem 500). The shifts in surface plasmon resonance (SPR) spectrum was determined by UV-visible spectrophotometer (Shimadzu UV-1800).

Fourier Transform Infrared Spectra analysis were carried out with Pelkin Elmer Spectrum Two equipped with ATR apparatus within the spectral region of

4000-400 cm^{-1} wave number at room temperature. Samples were scanned 4 times at a resolution of 2 cm^{-1} to get average spectra. To obtain FTIR spectra of samples, two drops of solution located on the crystal and the solvent were evaporated to eliminate solvent peaks from the spectra of the samples. FTIR spectra of $AuNP_{20}$, $AuNP_{23}$-PEI, $AuNP_{24}$-PEG, $AuNP_{50}$, $AuNP_{56}$-PEI and $AuNP_{57}$-PEG were obtained and analyzed.

Animals

A total of 21 male adult BALB/c mice were used for all the in vivo biochemical analysis. All the animal procedures were performed by virtue of Istanbul Medipol University Institutional Animal Care and Use Committee (IMU-HADYEK, Approval date/number: May 18, 2017 / 21). For the biochemical analysis, all the AuNP groups were dissolved in sterile PBS (250 µl) and injected as a single high dose (5 mg Au/kg animal weight) from the tail vein of the mice. All the mice were allowed free access to drinking water and diet. The cages were located in temperature-controlled normal room conditions and a light:dark period of 12 h.

Biochemical Analysis

The effects of various AuNPs groups on the changes in selected biochemical parameters (including; hemogram values, creatinine, alanine aminotransferase-ALT, aspartate aminotransferase-AST, total antioxidant capacity-TAC, total oxidant status-TOS) in mice were investigated. For this purpose, blood samples were collected via cardiac puncture which is considered a euthanasia procedure and should be performed only after ensuring that the animal was under deep anesthesia, from the mice 14 days post injection. Serum and plasma samples were obtained quickly by centrifugation at 3000 rpm for 10 min. Creatinin levels were measured with Jaffe method, and also ALT/AST parametres were measured with colorimetric method by the fully automatic analyzer (ROCHE module Cobas 6000), and the kits were procured by ROCHE. Hemogram values were analyzed with flow cytometry method by using hematology analyzer system (SYSMEX XN 1000).

The TAC and TOS values were measured colorimetrically in the mice serums using the methods developed by Erel [24, 25]. The principle of TAC measurement is briefly as follows: ABTS [2,2′-azinobis (3-ethylbenzothiazoline-6-sulfonic acid)] (Sigma-Aldrich) reagent is made radical with hydrogen peroxide by keeping the pH of the environment constant in the presence of acetate buffer (Sigma-Aldrich) solution. Following the addition of serum, antioxidants in the serum neutralize the existing ABTS radicals. As a result, the solution's color becomes lighter and the absorbance is measured at 658 nm. The principle of TOS measurement is briefly as follows: Fe_2SO_4 (Sigma-Aldrich) dissolves in water and releases Fe^{2+} ions. The oxidants in the serum enable Fe^{2+} to be oxidized to Fe^{3+}. The X-orange reagent (Sigma-Aldrich) used gives a colored complex with Fe^{3+}. The absorbance is measured at 658 nm. After TAC and TOS values are obtained, oxidative stress index (OSI) is calculated using the formula (TOS) / (TAC × 10).

Statistical Analysis

All the measurement and analysis results were given in tables. The numerical results represented the average values of three replicate measurements. Only the measurement results in the confidence interval of the device were used. No additional statistical approaches were used for differences between groups. Due to the large number of measured parameters, differences between the groups were discussed in the text.

RESULTS

Characterization of the AuNPs

The main characteristic properties of the synthesized gold nanoparticle groups are shown in Table 1. Seed gold nanoparticles ($AuNP_{20}$) were synthesized by the modified Turkevich method and were used in the synthesis of nanoparticles with the medium size ($AuNP_{50}$).

The gold nanoparticle size increased depending on the PEI and PEG surface functionalizations. Additionally, the polydispersity index (PDI) values remained below 0.2, showing highly monodisperse level. The changes in UV-visible peaks for seed and medium sized AuNRs occurred depending on the surface coatings. After the PEI coating, there was a significant positive increase in the zeta potentials. On the other hand, after the PEG coating, the zeta potential values re-

Table 1. Main characteristic properties of synthesized gold nanoparticle groups

AuNP Groups	Hydrodynamic diameter (nm)	Polydispersity index	UV-visible peak (nm)	Zeta potential (mV)
$AuNP_{20}$	20.04 ± 0.17	0.11	520	-48.53
$AuNP_{23}$-PEI	23.53 ± 0.20	0.15	522	+32.25
$AuNP_{24}$-PEG	24.92 ± 0.30	0.17	523	-22.76
$AuNP_{50}$	50.74 ± 0.14	0.12	535	-38.15
$AuNP_{56}$-PEI	56.21 ± 0.20	0.14	538	+30.16
$AuNP_{57}$-PEG	57.35 ± 0.30	0.16	540	-32.17

AuNP = gold nanoparticles, PEI = polyethyleneimine, PEG = polyethylene glycol

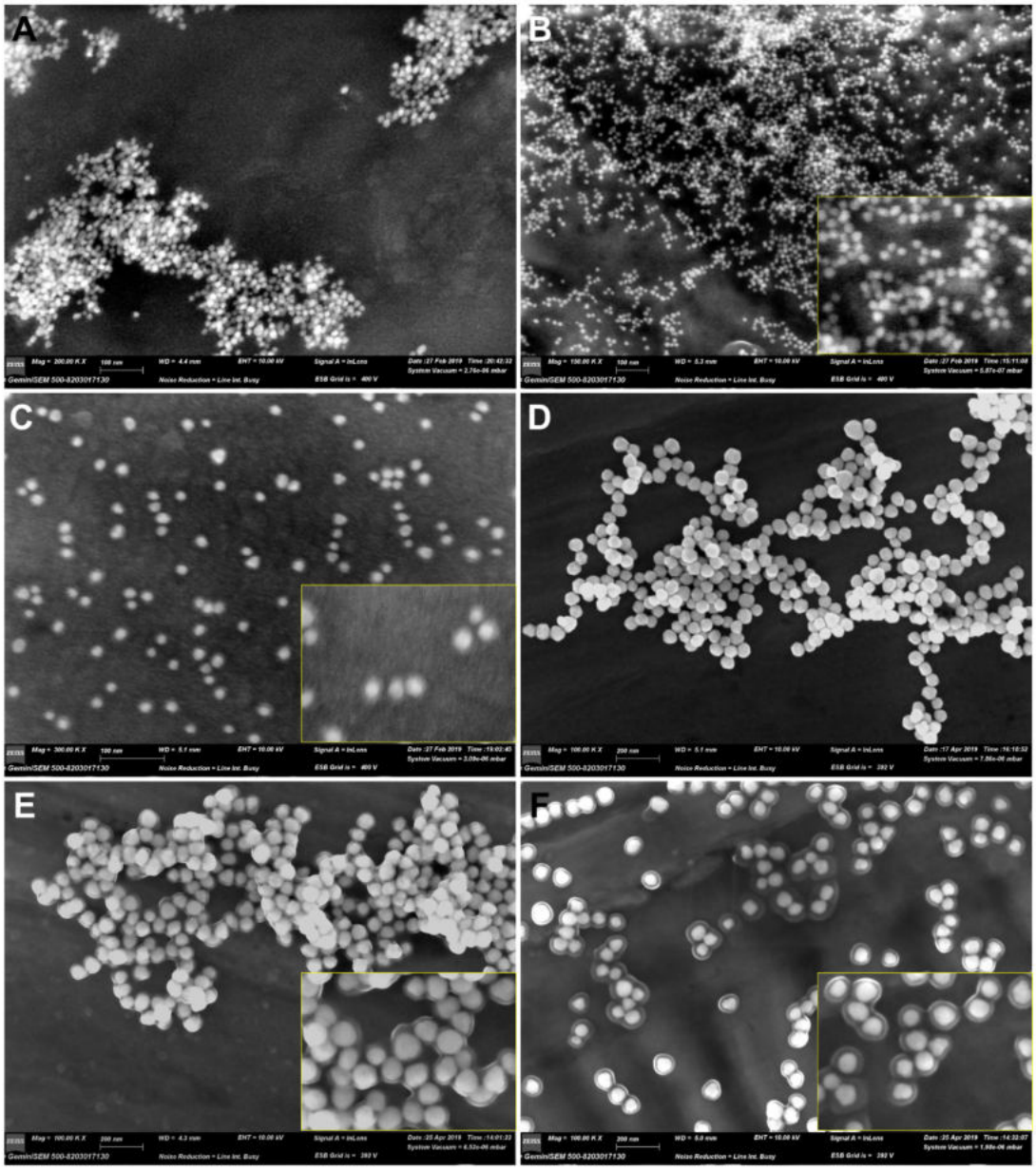

Fig. 1. SEM images of synthesized gold nanoparticles. (A) AuNP20. (B) $AuNP_{23}$-PEI. (C) $AuNP_{24}$-PEG. (D) $AuNP_{50}$. (E) $AuNP_{56}$-PEI. and (F) $AuNP_{57}$-PEG. AuNP = gold nanoparticles, PEI = polyethyleneimine, PEG = polyethylene glycol.

mained as negative (Table 1). According to the SEM images shown in Fig. 1, it is seen that highly monodisperse and stable gold nanoparticles have been synthesized. Again, the size measurements were also verified based on the SEM images. The PEI and PEG surface coatings are clearly visible, especially for the medium sized AuNPs (Figs. 1E and 1F). As shown in Figs. 1B and 1E, when AuNP was covered with PEI molecules, FTIR spectra of $AuNP_{23}$-PEI and $AuNP_{56}$-PEI yielded similar bands as PEI. The C-H stretching bands and N-H bending bands were observed at 1116 cm^{-1} and at 1574 cm^{-1} respectively which are similar to the positions observed with PEI. The peak at 3276 cm-1 and the shoulder at 3344 cm^{-1} are N-H stretching bands. The characteristic C-H stretching band is located at 2813 cm-1 [26]. The similar bands as PEG were shown in Figs. 1C and 1F. PEG, $AuNP_{24}$-PEG and $AuNP_{57}$-PEG spectrum peaks observed at 2883 cm^{-1} and 2971 cm^{-1} represent -CH_2 and -CH_3 asymmetrical vibrations respectively, whereas the peaks at 1115 cm-1 show -OH asymmetrical vibrations (Fig. 2) [27].

The Effects of the AuNPs on the Various Biochemical Parameters

The effects of different AuNP groups on the changes in the selected biochemical parameters in the mice were investigated on day 14 after a single i.v. injection (5 mg Au/kg animal weight) of the gold nanoparticle groups (Table 2). All the biochemical investigations were carried out using AuNP groups at a considerably higher dose than the literature. Significant changes in the biochemical parameters were observed depending on the surface coatings of the gold nanoparticles. Up to two-fold increases in the leukocyte percentages were observed compared to the control group with no AuNPs exposure. Additionally, PEI and PEG surface coatings slightly reduced this excessive increase. When the hemogram data were evaluated in terms of other standart parameters, generally the values were observed closer to the control group in the AuNP-PEI and AuNP-PEG groups.

According to the results of creatinine analysis applied to investigate kidney function, it was observed that the values increased up to two times compared to the control group. Nevertheless, it was evaluated that the values especially in PEI coated AuNP groups were closer to the control group. The liver, which is the organ where nanomaterial accumulates the most, is also very important in terms of nanotoxicity evaluations. The measured ALT and AST values were similar to the results of the cretain analysis. Additional surface coatings of the AuNPs (especially in the PEI groups) significantly reduced the excessive rise of these values. The ALT and AST levels excessively increased in direct relation to liver dysfunctions in the $AuNP_{20}$ and $AuNP_{50}$ groups. The TAC, TOS and OSI values measured as a result of these two values were generally considered to be close to each other. No excessive oxidative stress response was observed in all the gold nanoparticle groups. Again, TAC and TOS values in the surface functionalized AuNP groups were closer to the control group. Generally, in terms of all the bio-

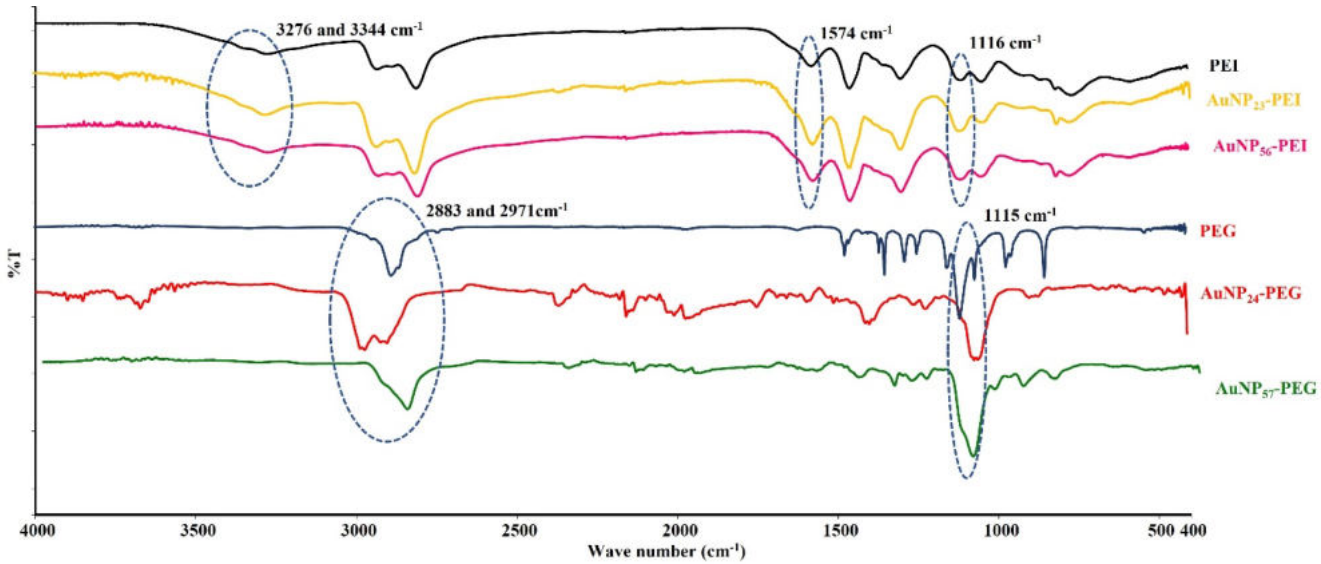

Fig. 2. FTIR-ATR analysis. FTIR = Fourier Transform Infrared, ATR = Attenuated Total Reflection.

Table 2. Effects of the AuNPs over the different biochemical parameters of the mice on day 14 after a single i.v. injection (5 mg Au/kg animal weight) of the gold nanoparticle groups

Biochemical parameters	Control	$AuNP_{20}$	$AuNP_{23}$ PEI	$AuNP_{24}$ PEG	$AuNP_{50}$	$AuNP_{56}$PEI	$AuNP_{57}$PEG
Leukocyte (%)	5.49	7.34	6.72	6.90	10.71	8.28	9.01
Erythrocyte (%)	4.82	4.43	4.83	4.77	3.22	4.98	4.99
Hemoglobin (g/dl)	13.49	10.20	14.60	14.40	9.80	13.40	13.60
Hematocrit (%)	40.00	34.00	43.60	41.60	29.20	42.30	42.10
MCV (μm^3)	86.00	76.70	87.20	90.30	84.40	84.90	90.70
PLC ($10^3/mm^3$)	270.00	207.00	264.00	239.00	201.00	282.00	251.00
RCDW (%)	14.11	13.20	17.10	13.10	14.50	14.20	13.00
PDW (%)	11.90	11.70	14.70	11.40	14.10	11.80	10.40
MPW (%)	11.40	9.90	11.50	10.00	9.40	11.40	10.00
Creatinin (mg/dl)	0.92	1.22	1.17	1.18	1.95	1.42	1.84
ALT (U/L)	36.15	71.40	44.80	64.40	76.00	68.10	75.00
AST (U/L)	159.25	272.20	184.90	243.70	352.40	257.40	298.00
TAC (mmol Trolox Equiv.)	0.43	0.53	0.43	0.46	0.62	0.56	0.60
TOS (µmol H_2O_2 Equiv.)	18.40	23.20	22.40	21.60	27.20	26.40	24.40
OSI	4.26	4.36	5.19	4.73	4.39	4.72	4.07

AuNP = gold nanoparticles, PEI = polyethyleneimine, PEG = polyethylene glycol, MCV = Mean cell volume, PLC = Platelet count, RCDW = Red cell distribution width, PDW = Platelet distribution width, MPV = Mean platelet volume, ALT = Alanine aminotransferase, AST = Aspartate aminotransferase, TAC = Total antioxidant capacity, TOS = Total oxidant status, OSI = Oxidative stress index.

chemical data, the PEI coating was evaluated to be more advantageous than the PEG coating.

DISCUSSION

Two different sizes of gold nanoparticles ($AuNP_{20}$ and $AuNP_{50}$) were successfully synthesized by the modified Turkevich method and seeding-growth method. Highly stable and monodisperse AuNPs were obtained. PEI and PEG surface coatings of the AuNPs made the nanostructures more stable, additionally prevented the aggregation of the particles. The particle sizes increased depending on the PEI and PEG surface modifications. Especially, after the PEI coating, there was a significant positive increase in the zeta potentials. Gold nanoparticles have a strong binding affinity to chemical groups such as; amine, thiol and disulfide. In this approach, nanoparticles can be easily physically modified with various polymers or biomolecules without the need for covalent bonds [28, 29]. In the protocol we followed, the PEI coating was carried out as a thin layer after synthesis under highly controlled conditions. In the PEG coating, polymer containing thiol group was used and an increased chemical stability was successfully achieved again. Positively charged nanoparticles could easily interact electrostatically with negatively charged molecules such as DNA and RNA directly. As this situation may facilitate DNA or RNA transfer, this is a great advantage for potential nanotherapeutic areas such as gene delivery, gene silencing and other molecular therapies [30-33].

Foreign molecules in the bloodstream are recognized by reticuloendothelial system (RES) elements through the opsonization process. The foreign substances are then transported to the liver and spleen by coating with antibodies for inactivation process [34]. After the intestinal nanomaterial absorption, significant accumulation occurs in the liver and spleen, followed by the kidneys and circulatory system [35]. As a result of i.v. injection of the AuNPs to mice with a single high dose (5 mg Au/kg animal weight) through

the tail vein, the various biochemical effects of particle groups were investigated on day 14. When the biochemical blood analysis data were evaluated, significant changes were observed depending on the surface coatings of the gold nanoparticles. Generally, in the AuNP-PEI and AuNP-PEG groups, the biochemical values were observed closer to the control group. PEI and PEG surface coatings increased biocompatibility. No excessive oxidative stress response was observed in all the AuNP groups. It has been evaluated that the surface chemistry of the particles is a more decisive parameter than the size over the biochemical toxicity in our study. Unlike our results, Lopez-Chaves *et al*. demonstrated that smaller particles lead to more toxic effects after the I.P. injection of the AuNPs of different diameters (10, 30 and 60 nm in sizes) to Wistar rats [36].

In terms of all the biochemical data in our study, the PEI functionalization was considered to be more advantageous than the PEG coating. In a study using glutathione coated AuNPs of 1.2 nm in diameter as an alternative to PEG coating, the researchers have demonstrated a low toxicity and immune response over the 4-weeks after the subcutaneous administration to the BALBc/cAnNHsd mice [37].

In the literature, it is seen that similar results were obtained in some studies using gold nanorods (AuNRs). After intratumoral injection of PEG-functionalized gold nanorods in cats and dogs, the researchers showed that the surface-modified nanostructures did not adversely affect biochemical blood parameters, kidney and liver functions within one-month period [38]. In another study evaluating the in vivo effects of PEG coated AuNRs functionalized with RGD and GLF, it was interestingly shown that PEG coated nanostructures increased ALT levels more than CTAB stabilized ones [39].

In a gold nanoparticle study, the *in vivo* toxic effects of CALNN pentapeptide coated AuNPs of 20 nm in diameter have been evaluated in a long period of 28 days. As a result of administration of a single dose (0.7 mg Au/kg of body weight) intravenously of the AuNPs to the rats, Fraga *et al*. showed that the ratio of red blood cells and hemoglobin/hematocrit levels decreased significantly. They evaluated the other hemogram values as normal [40]. Based on all these results; the surface coating, size, stability and biocompatibility of the AuNPs are important parameters for the potential biomedical applications of gold nanoparticles in future studies.

Limitations

The limitation of this study was that the biochemical analyses were carried out for only one day (day 14) due to the insufficient number of animals. If the measurement days could be determined for short and long time period, time dependent effects of the nanoparticles could be investigated as well.

CONCLUSION

In summary, we have performed a multiparametric study to understand the biochemical effects of the gold nanoparticles with different surface coatings and sizes in the mice. It has been concluded that the surface chemistry of the particles is more decisive parameter than the size in terms of in vivo toxicity. PEI and PEG surface coatings increased biocompatibility. No excessive oxidative stress response was observed in all the AuNP groups. Generally, it has been evaluated that PEI surface functionalization is more advantageous than PEG coating for potential in vivo applications. The surface modification, stability and biocompatibility of the AuNPs are important parameters for the biomedical applications of gold nanoparticles in future studies.

Authors' Contribution

Study Conception: İÖ; Study Design: İÖ, ÇÇ; Supervision: İÖ; Funding: İÖ; Materials: İÖ, ÜCE; Data Collection and/or Processing: İÖ, ÇÇ, NA, ÜCE; Statistical Analysis and/or Data Interpretation: İÖ, ÇÇ, NA; Literature Review: İÖ, ÜCE; Manuscript Preparation: İÖ and Critical Review: İÖ.

Conflict of interest

The authors disclosed no conflict of interest during the preparation or publication of this manuscript.

Financing

The authors would like to thank the Scientific and Technological Research Council of Turkey (Grant no: 217S135) for providing financial support to this Project.

REFERENCES

1. Boisselier E, Astruc D. Gold nanoparticles in nanomedicine: preparations, imaging, diagnostics, therapies and toxicity. Chem Soc Rev 2009;38:1759-82.
2. Hameed S, Wang Y, Zhao L, Xie L, Ying Y. Shape-dependent significant physical mutilation and antibacterial mechanisms of gold nanoparticles against foodborne bacterial pathogens (Escherichia coli, Pseudomonas aeruginosa and Staphylococcus aureus) at lower concentrations. Mater Sci Eng C Mater Biol Appl 2020;108:110338.
3. Hamdy ME, Del Carlo M, Hussein HA, Salah TA, El-Deeb AH, Emara MM, et al. Development of gold nanoparticles biosensor for ultrasensitive diagnosis of foot and mouth disease virus. J Nanobiotechnology 2018;16:48.
4. Camilo DE, Miyazaki CM, Shimizu FM, Ferreira M. Improving direct immunoassay response by layer-by-layer films of gold nanoparticles - Antibody conjugate towards label-free detection. Mater Sci Eng C Mater Biol Appl 2019;102:315-23.
5. Kwon SP, Jeon S, Lee SH, Yoon HY, Ryu JH, Choi D, et al. Thrombin-activatable fluorescent peptide incorporated gold nanoparticles for dual optical/computed tomography thrombus imaging. Biomaterials 2018;150:125-36.
6. Elbakry A, Wurster EC, Zaky A, Liebl R, Schindler E, Bauer-Kreisel P, et al. Layer-by-layer coated gold nanoparticles: size-dependent delivery of DNA into cells. Small 2012;8:3847-56.
7. Perche F, Yi Y, Hespel L, Mi P, Dirisala A, Cabral H, et al. Hydroxychloroquine-conjugated gold nanoparticles for improved siRNA activity. Biomaterials 2016;90:62-71.
8. Kalimuthu K, Lubin BC, Bazylevich A, Gellerman G, Shpilberg O, Luboshits G, et al. Gold nanoparticles stabilize peptide-drug-conjugates for sustained targeted drug delivery to cancer cells. J Nanobiotechnology 2018;16:34.
9. Ruttala HB, Ramasamy T, Poudel BK, Ruttala RRT, Jin SG, Choi HG, et al. Multi-responsive albumin-lonidamine conjugated hybridized gold nanoparticle as a combined photothermal-chemotherapy for synergistic tumor ablation. Acta Biomater 2020;101:531-43.
10. Hu K, Chen X, Chen W, Zhang L, Li J, Ye J, et al. Neuroprotective effect of gold nanoparticles composites in Parkinson's disease model. Nanomedicine 2018;14:1123-36.
11. Fratoddi I, Venditti I, Cametti C, Russo MV. How toxic are gold nanoparticles? The state-of-the-art. Nano Res 2015;8:1771-99.
12. Brandenberger C, Muhlfeld C, Ali Z, Lenz AG, Schmid O, Parak WJ, et al. Quantitative evaluation of cellular uptake and trafficking of plain and polyethylene glycol-coated gold nanoparticles. Small 2010;6:1669-78.
13. Zhao F, Zhao Y, Liu Y, Chang X, Chen C, Zhao Y. Cellular uptake, intracellular trafficking, and cytotoxicity of nanomaterials. Small 2011;7:1322-37.
14. Wang X, Hu X, Li J, Russe AC, Kawazoe N, Yang Y, et al. Influence of cell size on cellular uptake of gold nanoparticles. Biomater Sci 2016;4:970-8.
15. Stojiljkovic A, Kuehni-Boghenbor K, Gaschen V, Schupbach G, Mevissen M, Kinnear C. et al. High-content analysis of factors affecting gold nanoparticle uptake by neuronal and microglial cells in culture. Nanoscale 2016; 8:6650-16661.
16. Yu M, Lei B, Gao C, Yan J, Ma PX. Optimizing surface-engineered ultra-small gold nanoparticles for highly efficient miRNA delivery to enhance osteogenic differentiation of bone mesenchymal stromal cells. Nano Res 2016;10:49-63.
17. Shahbazi R, Ozcicek I, Ozturk G, Ulubayram K. Functionalized gold nanoparticles manifested as potent carriers for nucleolar targeting. Nanotechnology 2017;28:025103.
18. Ozcicek I, Aysit N, Cakici C, Aydeger A. The effects of surface functionality and size of gold nanoparticles on neuronal toxicity, apoptosis, ROS production and cellular/suborgan biodistribution. Mater Sci Eng C Mater Biol Appl 2021;128:112308.
19. Ozcicek I, Aysit N, Cakici C, Ayturk NU, Aydeger A, Erim UC. The effects of various surface coatings of gold nanorods on toxicity, neuronal localization, microstructural alterations, and in vitro/in vivo biodistribution. Adv Mater Interfaces 2022;9:2101369.
20. Khlebtsov N, Dykman L. Biodistribution and toxicity of engineered gold nanoparticles: a review of in vitro and in vivo studies. Chem Soc Rev 2011;40:1647-71.
21. Abdelhalim MAK, Jarrar BM. Histological alterations in the liver of rats induced by different gold nanoparticle sizes, doses and exposure duration. J Nanobiotechnol 2012;10:5.
22. Turkevich J, Stevenson PC, Hillier J. A study of the nucleation and growth processes in the synthesis of colloidal gold. Discuss Faraday Soc 1951:11:55
23. Perrault SD, Chan WCW. Synthesis and surface modification of highly monodispersed, spherical gold nanoparticles of 50-200 nm. J Am Chem Soc 2009;131:17042-3.
24. Erel O. A novel automated method to measure total antioxidant response against potent free radical reactions. Clin Biochem 2004;37:112-9.
25. Erel O. A new automated colorimetric method for measuring total oxidant status. Clin Biochem 2005;38:1103-11.
26. Cho TJ, Gorham JM, Pettibone JM, Liu JY, Tan JJ, V Hackley A. Parallel multiparameter study of PEI-functionalized gold nanoparticle synthesis for biomedical applications: Part 2. Elucidating the role of surface chemistry and polymer structure in performance. Langmuir 2020; 36:14058-69.
27. Shen CC, Hsu SH, Chang KB, Yeh CA, Chang HC, Tang CM, et al. Physical gold nanoparticle-decorated polyethylene glycol-hydroxyapatite composites guide osteogenesis and angiogenesis of mesenchymal stem cells. Biomedicines 2021 9:1632.
28. Katz E. and Willner I. Integrated nanoparticle-biomolecule hybrid systems: Synthesis, properties, and applications. Angew Chem Int Ed Engl 2004;43:6042-108.
29. Ojea-Jimenez I. Puntes V. Instability of cationic gold nanoparticle bioconjugates: the role of citrate ions. J Am Chem Soc 2009;131:13320-7.
30. Song WJ, Du JZ, Sun TM, Zhang PZ, Wang J. Gold nanoparticles capped with polyethyleneimine for enhanced siRNA delivery. Small 2010;6:239-46.
31. Lee Y, Lee SH, Kim JS, Maruyama A, Chen X, Park TG. Controlled synthesis of PEI-coated gold nanoparticles using re-

ductive catechol chemistry for siRNA delivery. J Control Release 2011;155:3-10.
32. Kong L, Qiu J, Sun W, Yang J, Shen M, Wang L, et al. Multifunctional PEI-entrapped gold nanoparticles enable efficient delivery of therapeutic siRNA into glioblastoma cells. Biomater Sci 2017;5:258-66.
33. Shahbazi R, Asik E, Kahraman N, Turk M, Ozpolat B, Ulubayram K. Modified gold-based siRNA nanotherapeutics for targeted therapy of triple-negative breast cancer. Nanomedicine 2017;12:1961-73.
34. Lasagna-Reeves C, Gonzalez-Romero D, Barria MA, Olmedo I, Clos A, Ramanujam VMS, et al. Bioaccumulation and toxicity of gold nanoparticles after repeated administration in mice. Biochem Bioph Res Co 2010;393:649-55.
35. Ganguly P, Breen A, Pillai SC. Toxicity of nanomaterials: exposure, pathways, assessment, and recent advances. Acs Biomater Sci Eng 2018;4:2237-75.
36. Lopez-Chaves C, Soto-Alvaredo J, Montes-Bayon M, Bettmer J, Llopis J, Sanchez-Gonzalez C. Gold nanoparticles: distribution, bioaccumulation and toxicity. In vitro and in vivo studies. Nanomedicine 2018;14:1-12.
37. Simpson CA, Salleng KJ, Cliffel DE, Feldheim DL. In vivo toxicity, biodistribution, and clearance of glutathione-coated gold nanoparticles. Nanomedicine 2013;9:257-63.
38. Abdoon A.S., Al-Ashkar E.A., Kandil O.M., Shaban A.M., Khaled H.M., El Sayed M.A., et al. Efficacy and toxicity of plasmonic photothermal therapy (PPTT) using gold nanorods (GNRs) against mammary tumors in dogs and cats. Nanomedicine 2016;12:2291-7.
39. Bartneck M, Ritz T, Keul HA, Wambach M, J Bornemann, Gbureck UJ, et al. Peptide-functionalized gold nanorods increase liver injury in hepatitis. Acs Nano 2012;6:8767-77.
40. Fraga S, Brandao A, Soares ME, Morais T, Duarte JA, Pereira L, et al. Short- and long-term distribution and toxicity of gold nanoparticles in the rat after a single-dose intravenous administration. Nanomedicine 2014;10:1757-66.